Nanostructures

DOI: 10.1002/anie.200603309

Preparation and Electrochemical Properties of SnO_2 Nanowires for Application in Lithium-Ion Batteries**

*Min-Sik Park, Guo-Xiu Wang, Yong-Mook Kang, David Wexler, Shi-Xue Dou, and Hua-Kun Liu**

One-dimensional (1D) nanostructured materials have received considerable attention for advanced functional systems as well as extensive applications owing to their attractive electronic, optical, and thermal properties.[1–2] In lithium-ion-battery science, recent research has focused on nanoscale electrode materials to improve electrochemical performance. The high surface-to-volume ratio and excellent surface activities of 1D nanostructured materials have stimulated great interest in their development for the next generation of power sources.[3–4]

Materials based on tin oxide have been proposed as alternative anode materials with high-energy densities and stable capacity retention in lithium-ion batteries.[5–7] Various SnO_2-based materials have displayed extraordinary electrochemical behavior such that the initial irreversible capacity induced by Li_2O formation and the abrupt capacity fading caused by volume variation could be effectively reduced when in nanoscale form.[8–10] From this point of view, SnO_2 nanowires can also be suggested as a promising anode material because the nanowire structure is of special interest with predictions of unique electronic and structural properties. Furthermore, the nanowires can be easily synthesized by a thermal evaporation method. However, in its current form, this method of manufacture of SnO_2 nanowires has several limitations: it is inappropriate for mass production as high synthesis temperatures are required and there are difficulties in the elimination of metal catalysts that could act as impurities or defects. This results in reversible capacity loss or poor cyclic performance during electrochemical reactions.[11,12] The critical issues relating to SnO_2 nanowires as anode materials for lithium-ion batteries are how to avoid the deteriorative effects of catalysts and how to increase production.

Herein, we report on the preparation and electrochemical performance of self-catalysis-grown SnO_2 nanowires to determine their potential use as an anode material for lithium-ion batteries. SnO_2 nanowires have been synthesized by thermal evaporation combined with a self-catalyzed growth procedure by using a ball-milled evaporation material to increase production at lower temperature and prevent the undesirable effects of conventional catalysts on electrochemical performance. The self-catalysis-grown SnO_2 nanowires show higher initial coulombic efficiency and an improved cyclic retention compared with those of SnO_2 powder and SnO_2 nanowires produced by Au-assisted growth.[11]

The self-catalysis growth method, which uses a ball-milled mixture of SnO and Sn powder as an evaporation source, is appropriate for obtaining SnO_2 nanowires with high purity. The deposited products on the Si substrates contain almost 100% of the SnO_2 nanowires formed. Observation with scanning electron microscopy (SEM) clearly shows a general view of randomly aligned SnO_2 nanowires with diameters of 200–500 nm and lengths extending to several tens of micrometers (Figure 1a). Sn droplets at the tips of nanowires were observed and confirmed by energy dispersive X-ray (EDX)

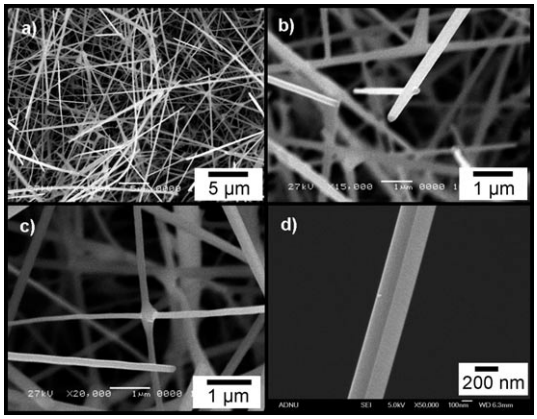

Figure 1. The microstructure of self-catalysis-grown SnO_2 nanowires. a) SEM image of SnO_2 nanowires; b) SEM image of tips including Sn droplets; c) SEM image of junction; and d) field-emission SEM (FESEM) image of an individual nanowire stem.

[*] M.-S. Park, Prof. S.-X. Dou, Prof. H.-K. Liu
Institute for Superconducting and Electronic Materials and
ARC Centre of Excellence for Electromaterials Science
University of Wollongong
Wollongong, NSW 252 (Australia)
Fax: (+61) 242-215-731
E-mail: hua_liu@uow.edu.au
Homepage: http://www.uow.edu.au/eng/research/ISEM/
Dr. Y.-M. Kang
Energy Lab
Samsung SDI Co., Ltd.
428-5, Gongse-ri, Giheung-eup
Yongin-si, Gyeonggi-do (Republic of Korea)
Dr. G.-X. Wang, Dr. D. Wexler
School of Mechanical Materials and Mechatronic Engineering
University of Wollongong
Wollongong, NSW 2522 (Australia)

[**] Financial support provided by the Australian Research Council (ARC) through the ARC Centre of Excellence (CE0561616) and ARC Discovery (DP0559891) are gratefully acknowledged. The authors thank Dr. T. Silver at the University of Wollongong and Prof. J. H. Ahn at Andong National University.

Supporting information for this article is available on the WWW under http://www.angewandte.org or from the author.

spectroscopy (Figure 1b and c). In regards to the low melting point of Sn (231.9 °C), it is suggested that Sn particles in the starting material form liquid nuclei on the Si substrate at the initial stage of the evaporation above 300 °C, leading to vapor–liquid–solid (VLS) growth of the SnO_2 nanowires at 900 °C. The Sn droplets were essential for growth of SnO_2 nanowires without conventional catalysts and for determining the diameters of nanowires. More interestingly, close inspection of the stem of an individual nanowire showed a quadrilateral cross-section (Figure 1d), which is in agreement with a tetragonal structure.

Figure 2a shows an X-ray diffraction (XRD) pattern of SnO_2 nanowires compared with that of SnO_2 powder. All reflections of SnO_2 nanowires are in excellent accordance with a tetragonal rutile structure (JCPDS 41-1445), which

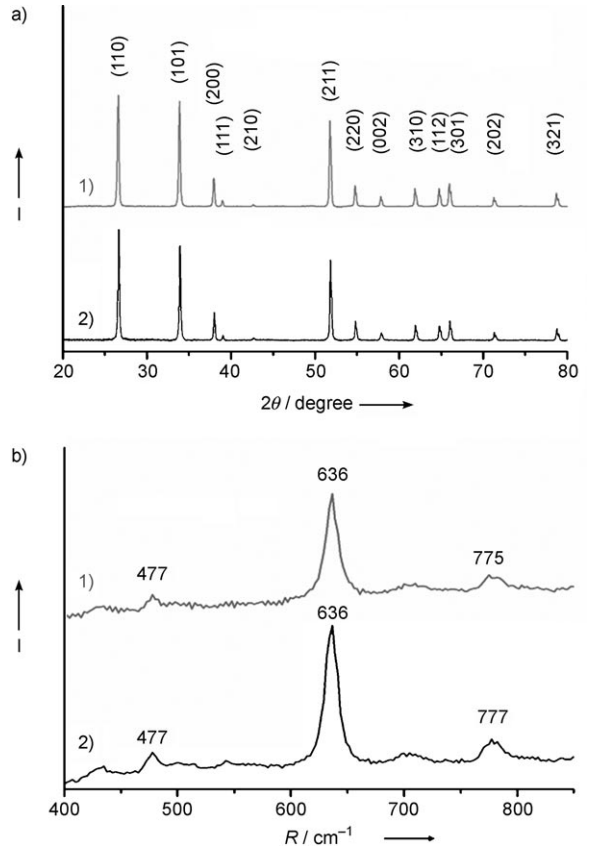

Figure 2. a) X-ray diffraction patterns of SnO_2 nanowires (1) and SnO_2 powder (2). b) Room-temperature Raman spectra of SnO_2 nanowires (1) and SnO_2 powder (2). I = intensity, R = Raman shift.

belongs to the space group $P4_2/mnm$ (number 136). The lattice parameters of the nanowires were $a = b = 4.738$ Å and $c = 3.188$ Å. It is well known that a nanowire form with a high aspect ratio experiences more tensile stress along the c axis direction on the surface than the powder form, which leads to an increase in the c value. In accord with this, c-axis-related peak shifts to lower angles were detected for SnO_2 nanowires when compared with the powder; the shifts of the nanowires were $\Delta(2\theta) = 0.063°$, 0.067°, and 0.058° for the (101), (002), and (301) peaks, respectively. The full width at half maximum (FWHM) of the (002) peak for SnO_2 nanowires and SnO_2 powder were calculated to be 0.2800° and 0.3400°, respectively. The apparently smaller FWHM for the (002) peak indicates that the nanowires have better crystallinity with fewer lattice distortions along the c axis in the tetragonal system. From the XRD results, the c-axis-related peak shifts and FWHM behavior provided evidence of an increase in the c axis parameter in the nanowire lattice structure. Figure 2b shows Raman spectra of the SnO_2 nanowires compared with SnO_2 powder. The fundamental Raman scattering peaks for SnO_2 powder were observed at 477 cm^{-1}, 636 cm^{-1}, and 777 cm^{-1}, corresponding to the E_g, A_{1g}, and B_{2g} vibration modes, respectively.[9] We also found these peaks in the Raman spectra of SnO_2 nanowires at 477 cm^{-1}, 636 cm^{-1}, and 775 cm^{-1}. The downwards shift of the B_{2g} vibration mode for SnO_2 nanowires could be caused by the size effect of the structure.[12] These results are also consistent with formation of self-catalysis-grown SnO_2 nanowires with a single crystalline structure.

TEM bright-field imaging combined with selected-area diffraction (SAD) revealed the fine microstructure of the SnO_2 nanowires, each wire being a monocrystal with a tetragonal structure (Figure 3a). Tilting experiments also

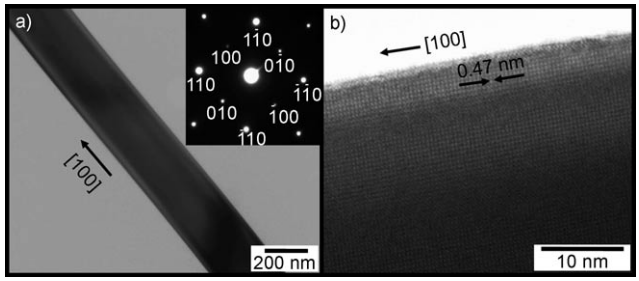

Figure 3. a) TEM image and SAD patterns (inset) of a SnO_2 nanowire. Zone axis is [001]. b) HRTEM image of a section of a SnO_2 nanowire.

revealed no evidence of extended defects within the individual crystals. High-resolution (HR) imaging was combined with SAD to investigate the nanowire growth direction. For the wire shown in Figure 3a, the zone axis is [001] and the growth direction of the nanowire is parallel to [100]. The HRTEM image (Figure 3b) confirms this, with an interplanar spacing of approximately 0.47 nm between neighboring [100] planes of tetragonal SnO_2.

The anodic performance of SnO_2 nanowires was tested in the potential range of 0.05 to 1.5 V (versus Li/Li^+). For comparative purposes, SnO_2 powder was also examined under the same conditions. The SnO_2 nanowires show much higher Li^+ storage and a relatively smaller initial irreversible capacity of 1134 mAh g^{-1} in the galvanostatic voltage profiles for the first cycle, as shown in Figure 4a. Note that the SnO_2 nanowires show an initial coulombic efficiency of approximately 46.91 %, which is notably higher than that of the SnO_2 powders (31.01 %). The improvement of electrochemical

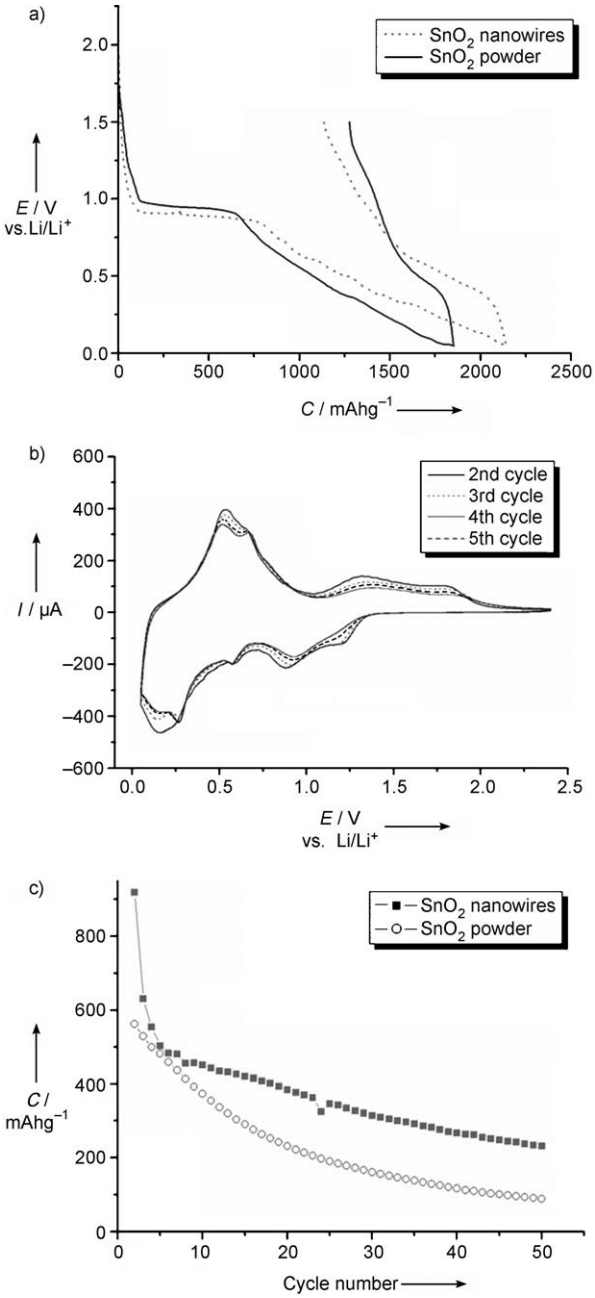

Figure 4. The anodic performance of the SnO_2 nanowires. a) The galvanostatic voltage profile (C = capacity, E = potential) for the first cycle between 0.05 V and 1.5 V compared with pure SnO_2 powder. b) Cyclic voltammograms from the second cycle to the fifth cycle at a scan rate of 0.05 $mV s^{-1}$ in the voltage range of 0.05–2.5 V. c) The cyclic performance from the second cycle to the 50th cycle of SnO_2 nanowires and pure SnO_2 powder at the same current density, 100 $mA g^{-1}$. C = discharge capacity.

behavior should be attributed to the 1D nanowire structure with a large surface area and high length/diameter ratio. The 1D nanowire structure could provide more reaction sites on the surface, and the smaller diameter of the nanowires provides a short diffusion length for Li^+ insertion, which could enhance the charge transfer and electron conduction along the length direction. More importantly, the Sn droplets on the tips of nanowires could also contribute to the Li^+ storage and reduce the pulverization owing to lattice mismatches at the interfaces between nanowires and catalysts, which would result in improvements in the initial coulombic efficiency and Li^+ storage. To identify electrochemical reactions during cycles, cyclic voltammograms (CV) of SnO_2 nanowires were obtained and are presented in Figure 4b. The CV profiles show two apparent reduction peaks around 0.95 V and 1.20 V derived from Li_2O formation and electrolyte decomposition when SnO_2 nanowires react with Li^+ as described in Equation (1).[8] These peaks should disappear, leaving a

$$SnO_2 + 4\,Li^+ + 4\,e^- \rightarrow Sn + 2\,Li_2O \qquad (1)$$

large initial irreversible capacity after the first cycle in SnO_2 powder electrodes. However, these irreversible reactions were still taking place until the fifth cycle in SnO_2 nanowire electrodes. We suggest that the single-crystalline structure of nanowires may disturb smooth Li^+ insertion into the interior of the nanowires, which leads to a slow lithiation. Furthermore, the additional electrolyte decomposition on the new surface induced by volume expansion may result in irreversible capacity even after the first cycle. Based on these considerations, the Li_2O formation and electrolyte decomposition might continue through subsequent cycles, leading to an increasing irreversible capacity up to the fifth cycle, as shown in Figure 4c.

The other pairs of reduction and oxidation peaks at 0.25 V and 0.6 V during the discharge and at 0.5 V and 0.7 V during the charge cycles are related to the formation of Li_xSn as described in Equation (2).[8] The self-catalysis-grown SnO_2

$$Sn + x\,Li + x\,e^- \leftrightarrow Li_xSn \quad (0 \le x \le 4.4) \qquad (2)$$

nanowires exhibit improved cyclic performance and a higher reversible specific capacity of over 300 $mAh g^{-1}$ up to the 50th cycle as shown in Figure 4c. This suggests that the 1D nanowire structure with a high aspect ratio of length to diameter effectively increases the charge-transfer properties along the length direction compared with the powder form. Moreover, the self-catalysis-grown SnO_2 nanowires show a smaller capacity fading of 1.45% per cycle after the fifth cycle, which is much smaller than that of SnO_2 nanowires grown through Au assistance (3.89%).[11] It is likely that the reversible capacity loss or electrical disconnection induced by the traditional metal catalysts could be effectively reduced in the self-catalysis-grown SnO_2 nanowires.

In summary, we have fabricated self-catalysis-grown SnO_2 nanowires by a thermal evaporation process. The ball-milled evaporation source served to increase production and decrease the synthesis temperature. The Sn particles in the evaporation source played the role of the catalyst, allowing VLS growth of the SnO_2 nanowires. The 1D nanowire structure could provide more reaction sites on the surface and enhance the charge transfer in the electrochemical reactions. Moreover, Sn particles at the tips of nanowires also contributed to the Li^+ storage and prevented the capacity loss that is induced by the existing metal catalysts.

Experimental Section

The thermal evaporation process was employed to synthesize SnO_2 nanowires. As an evaporation source, high purity SnO (99.99%, Aldrich) and Sn (99.99%, Aldrich) powders were homogeneously mixed in a 1:1 weight ratio by a planetary mechanical milling process for 40 h under an atmosphere of argon. Ball-milled powder (1 g) was placed in an alumina boat located inside a tube furnace. Silicon substrates without metal catalysts were placed downstream one by one at a distance of about 15 cm from the powder. The heating temperature and time were optimized at 900 °C and 1 h, respectively. The deposition pressure was 100 Torr of high purity Ar gas at a flow rate of 50 sccm (standard cubic centimeters per minute). The morphology and microstructure of self-catalysis-grown SnO_2 nanowires were characterized by XRD (Philips 1730), SEM (JEOL JEM-3000), TEM (JEOL 2011), and Raman spectroscopy (Jobin Yvon HR800). The SnO_2 nanowires were mixed with acetylene black (AB) and a binder (poly(vinylidene fluoride); PVdF) at a weight ratio of 75:15:10, respectively, in a solvent (*N*-methyl-2-pyrrolidone). The slurry was uniformly pasted on Cu foil. Such prepared electrode sheets were dried at 120 °C in a vacuum oven and pressed under a pressure of approximately 200 $kg\,cm^{-2}$. CR2032-type coin cells were assembled for electrochemical characterization. The electrolyte was 1M $LiPF_6$ in a 1:1 mixture of ethylene carbonate and dimethyl carbonate. Li metal foil was used as the counter and reference electrode. The cells were galvanostatically charged and discharged at a current density of 100 $mA\,g^{-1}$ over a range of 0.05 V to 1.5 V.

Received: August 14, 2006
Revised: November 3, 2006
Published online: December 13, 2006

Keywords: electrochemistry · electron microscopy · lithium-ion batteries · nanostructures · tin oxide

[1] A. M. Morales, C. M. Lieber, *Science* **1998**, *279*, 208.
[2] Z. W. Pan, Z. R. Dai, Z. L. Wang, *Science* **2001**, *291*, 1947.
[3] C. Kim, M. Noh, M. Choi, J. Cho, B. Park, *Chem. Mater.* **2005**, *17*, 3297.
[4] C. R. Sides, C. R. Martin, *Adv. Mater.* **2005**, *17*, 125.
[5] Y. Idota, T. Kubota, A. Matsufuji, Y. Maekawa, T. Miyasaka, *Science* **1997**, *276*, 1395.
[6] J. O. Besenhard, J. Yang, M. Winter, *J. Power Sources* **2000**, *90*, 70.
[7] I. A. Courtney, J. R. Dahn, *J. Electrochem. Soc.* **1997**, *144*, 2045.
[8] N. Li, C. R. Martin, *J. Electrochem. Soc.* **2001**, *148*, A164.
[9] J. Fan, T. Wang, C. Yu, B. Tu, Z. Jiang, D. Zhao, *Adv. Mater.* **2004**, *16*, 1432.
[10] S. Han, B. Jang, T. Kim, S. M. Oh, T, Hyeon, *Adv. Funct. Mater.* **2005**, *15*, 1845.
[11] Z. Ying, Q. Wan, H. Cao, Z. T. Song, S. L. Feng, *Appl. Phys. Lett.* **2005**, *87*, 113108.
[12] I. H. Campbell, P. M. Fauchet, *Solid State Commun.* **1986**, *58*, 739.

